

---

EFDA–JET–CP(07)03/52

Y. Liang, H.R. Koslowski, P.R. Thomas, E. Nardon, S. Jachmich, B. Alper, P. Andrew, Y. Andrew, G. Arnoux, Y. Baranov, M. Bécoulet, M. Beurskens, T. Biewer, M. Bigi, K. Crombe, E. De La Luna, P. de Vries, T. Eich, H.G. Esser, W. Fundamenski, S. Gerasimov, C. Giroud, M.P. Gryaznevich, D. Harting, N. Hawkes, S. Hotchin, D. Howell, A. Huber, M. Jakubowski, V. Kiptily, A. Kreter, L. Moreira, V. Parail, S.D. Pinches, E. Rachlew, O. Schmitz, O. Zimmermann, and JET EFDA contributors

# Active Control of Type-I Edge Localized Modes on JET

"This document is intended for publication in the open literature. It is made available on the understanding that it may not be further circulated and extracts or references may not be published prior to publication of the original when applicable, or without the consent of the Publications Officer, EFDA, Culham Science Centre, Abingdon, Oxon, OX14 3DB, UK."

"Enquiries about Copyright and reproduction should be addressed to the Publications Officer, EFDA, Culham Science Centre, Abingdon, Oxon, OX14 3DB, UK."

# Active Control of Type-I Edge Localized Modes on JET

Y. Liang<sup>1</sup>, H.R. Koslowski<sup>1</sup>, P.R. Thomas<sup>2</sup>, E. Nardon<sup>2</sup>, S. Jachmich<sup>3</sup>, B. Alper<sup>4</sup>,  
P. Andrew<sup>4</sup>, Y. Andrew<sup>4</sup>, G. Arnoux<sup>2</sup>, Y. Baranov<sup>4</sup>, M. Bécoulet<sup>2</sup>, M. Beurskens<sup>4</sup>,  
T. Biewer<sup>5</sup>, M. Bigi<sup>6</sup>, K. Crombe<sup>7</sup>, E. De La Luna<sup>8</sup>, P. de Vries<sup>4</sup>, T. Eich<sup>9</sup>,  
H.G. Esser<sup>1</sup>, W. Fundamenski<sup>4</sup>, S. Gerasimov<sup>4</sup>, C. Giroud<sup>4</sup>, M.P. Gryaznevich<sup>4</sup>,  
D. Harting<sup>1</sup>, N. Hawkes<sup>4</sup>, S. Hotchin<sup>4</sup>, D. Howell<sup>4</sup>, A. Huber<sup>1</sup>, M. Jakubowski<sup>1</sup>,  
V. Kiptily<sup>4</sup>, A. Kreter<sup>1</sup>, L. Moreira<sup>4</sup>, V. Parail<sup>4</sup>, S.D. Pinches<sup>4</sup>, E. Rachlew<sup>10</sup>,  
O. Schmitz<sup>1</sup>, O. Zimmermann<sup>1</sup> and JET EFDA contributors\*

<sup>1</sup>*Forschungszentrum Jülich GmbH, Association EURATOM-FZ Jülich, Institut für Energieforschung-Plasmaphysik,  
Trilateral Euregio Cluster, D-52425 Jülich, Germany*

<sup>2</sup>*Association EURATOM-CEA, 13108 St Paul-lez-Durance, France*

<sup>3</sup>*Association EURATOM-Belgian State, Koninklijke Militaire School-Ecole Royale Militaire, B-1000 Brussels, Belgium*

<sup>4</sup>*EURATOM-UKAEA Fusion Association, Culham Science Centre, OX14 3DB, Abingdon, OXON, UK*

<sup>5</sup>*Oak Ridge National Laboratory, Oak Ridge, TN 37831, USA*

<sup>6</sup>*Associazione EURATOM-ENEA sulla Fusione, Consorzio RFX Padova, Italy*

<sup>7</sup>*Association EURATOM-Belgian State, Department of Applied Physics Ghent University, B-9000 Ghent, Belgium*

<sup>8</sup>*Asociación EURATOM-CIEMAT, Avenida Complutense 22, E-28040 Madrid, Spain*

<sup>9</sup>*Association EURATOM-Max-Planck-Institut für Plasmaphysik, D-85748 Garching, Germany*

<sup>10</sup>*Association EURATOM-VR, Department of Physics, SCI, KTH, SE-10691 Stockholm, Sweden*

\* See annex of M.L. Watkins et al, "Overview of JET Results",  
(Proc. 21<sup>st</sup> IAEA Fusion Energy Conference, Chengdu, China (2006)).

Preprint of Paper to be submitted for publication in Proceedings of the  
34th EPS Conference on Plasma Physics,  
(Warsaw, Poland 2nd - 6th July 2007)



## ABSTRACT.

The operational domain for active control of type-I Edge Localized Modes (ELMs) with an  $n = 1$  external magnetic perturbation field induced by the ex-vessel error field correction coils on JET has been developed toward more ITER relevant regimes with high plasma triangularity, up to 0.45, high normalized beta, up to 3.0, plasma current up to 2.0MA and  $q_{95}$  varied between 3.0 and 4.8. The results of ELM mitigation in high triangularity plasmas show that the frequency of type-I ELMs increased by a factor of 4 during the application of the  $n = 1$  fields, while the energy loss per ELM,  $\Delta W = W$ , decreased from 6% below the noise level of the diamagnetic measurement ( $< 2\%$ ). No reduction of confinement quality (H98Y) during the ELM mitigation phase has been observed. The minimum  $n = 1$  perturbation field amplitude above which the ELMs were mitigated increased with a lower  $q_{95}$  but always remained below the  $n = 1$  locked mode threshold. The first results of ELM mitigation with  $n = 2$  magnetic perturbations on JET demonstrate that the frequency of ELMs increased from 10Hz to 35Hz. and a wide operational window of  $q_{95}$  from 4.5 to 3.1 has been found.

## 1. INTRODUCTION

The foreseen ITER baseline operating scenario [1] is the type-I ELMy H-mode [2, 3]. The periodic and transient expulsion of energy onto plasma facing components, as extrapolated from current devices, is predicted to be too high and will pose a severe problem for the integrity and lifetime of these components [4]. Therefore, reliable methods to the control of ELM power losses are required.

Several possible active control mechanisms are presently under discussion: (i) edge ergodisation by resonant magnetic perturbations [5], (ii) pellet pace-making of ELMs [6], (iii) vertical plasma oscillations to trigger ELMs [7], or (iv) enhanced toroidal field ripple [8]. The effect of perturbing magnetic fields on the stability of ELMs has been investigated on several tokamaks [9, 10, 11]. Complete suppression of type-I ELMs has been demonstrated on DIII-D with resonant magnetic fields ( $n = 3$ ) [5]. All these experiments were carried out with perturbation fields created by in-vessel magnetic coils. In view of designing next generation tokamaks, ELM control through the application of low- $n$  perturbation fields generated by ex-vessel coil systems is an attractive solution that needs further exploration.

At JET, ELM mitigation experiments with low- $n$  External Magnetic Perturbation Fields (EMPFs) induced by the Error Field Correction Coils (EFCCs) mounted outside of the vacuum vessel were carried out successfully. The first results from this experiment showed that the frequency and the amplitude of type-I ELMs can be actively controlled by the application of an  $n = 1$  EMPF generated by the EFCCs [13]. During the application of the  $n = 1$  field the ELM frequency increased by a factor of 4 and the amplitude of the  $D\alpha$  signal decreased. The energy loss per ELM normalised to the total stored energy,  $\Delta W = W$ , decreased from 7% to less than 2%. ELM mitigation does not depend on the phase of the  $n = 1$  external fields. The pump-out effect [15], the reduction in ELM amplitude, the simultaneous increase in ELM frequency, and a reduction in fast ion losses were observed independent on the phase of the  $n = 1$  field. The temperature of the outer limiter dropped when the EFCCs were

applied. Transport analysis using the TRANSP code [14] shows that no or a modest reduction of the thermal energy confinement time,  $\tau_{\text{therm}}$ , because of the density pump-out, but when normalised to the IPB98(y,2) scaling [1] the confinement shows almost no reduction.

In this paper, further experimental investigations of the operational domain for active control of type-I ELMs with  $n = 1$  EMPFs in a more ITER relevant parameter space, i.e. at high triangularity and at high beta on JET are presented. Furthermore, the first experimental results of active ELM control using the  $n = 2$  EFCC configuration are described.

## 2. EXTERNAL MAGNETIC PERTURBATION FIELD INDUCED BY ERROR FIELD CORRECTION COILS ON JET

On JET, external perturbation fields can be applied by the EFCC [12]. The system consists of four square shaped coils ( $\sim 6$  m in dimension) which are mounted at equally spaced toroidal positions and attached to the transformer yokes as shown in Fig.1 (a) Each coil spans a toroidal angle of  $70^\circ$  and has a radial distance along the winding of 5.3 to 7m from the axis of the machine. It has 16 turns and the maximum total coil current amounts to  $I_{\text{EFCC}} = 48\text{kAt}$ . Here, the total current is given in terms of the current in one coil winding times the number of turns. Depending on the wiring of the EFCCs either  $n = 1$  or  $n = 2$  EMPFs can be created.

In fact, the EFCCs system on JET was originally designed for compensation in both amplitude and phase of the  $n = 1$  harmonic of the intrinsic error field arising from imperfections in the construction or alignment of the magnetic field coils [12]. Previous studies of the error field on JET show that the amplitude of the intrinsic error,  $B_{n=1}^{\text{err}}(q=2)=B$ , is only in the order of  $10^{-5}$  [17] which corresponds to few kAt of EFCC current.

The effective radial resonance magnetic perturbations,  $|b_{\text{res}}^{\text{r,eff}}| = |B_{\text{res}}^{\text{r,eff}}/B_0|$ , calculated for  $I_{\text{EFCC}} = 1\text{kAt}$  in both,  $n = 1$  and  $n = 2$  configurations are shown in Fig.1 (b), where  $B_{\text{r,eff res}}$  and  $B_0$  are the radial resonant magnetic perturbation field and the toroidal magnetic fields, respectively. In the  $n = 1$  EFCC configuration, the amplitude of the  $n = 1$  harmonic is one or two magnitudes larger than other components ( $n = 2, 3$ ). However, there is still an  $n = 1$  harmonic existing in the  $n = 2$  EFCC configuration due to the geometry of the EFCCs, and the amplitude of  $b^{\text{r,eff}}(n = 1)$  is similar to that of  $b^{\text{r,eff}}(n = 2)$  at the plasma edge. Although the amplitude of  $b^{\text{r,eff}}(n = 2)$  in  $n = 2$  EFCCs is by a factor of 3 smaller than  $b^{\text{r,eff}}(n = 1)$  in  $n = 1$  EFCCs, the number of resonant surfaces increased twice and the distances between resonant surfaces are reduced too. Here, the calculation is based upon an equilibrium reconstruction for Pulse No: 67954 shown in figure 1 of ref. [13] with the perturbing field in vacuum superimposed. Screening effects due to plasma rotation have been neglected.

## 3. EXTENSION OF THE OPERATIONAL DOMAIN FOR ELM MITIGATION WITH $n = 1$ EMPF

Recent experiments have shown that ELM mitigation with an  $n = 1$  field is applicable in high beta plasmas ( $\beta_N = 3$ ;  $B_t = 1.8\text{T}$  and  $I_p = 1.2\text{ MA}$ ) without causing a degradation of the thermal energy confinement time [16].

### 3.1. ELM MITIGATION WITH THE $n = 1$ EMPF IN HIGH TRIANGULARITY PLASMA

An overview on an ELM mitigation pulse is shown in Fig.2. The traces are: (a) the total input power,  $P_{\text{tot}}$ , and the total stored energy,  $E_{\text{dia}}$ , (b) upper and lower plasma triangularity,  $\delta_U$ ;  $\delta_L$ , (c)  $I_{\text{EFCC}}$ , (d) the line integrated electron densities  $n_e l$ , measured with an interferometer along two lines of sight, one close to the magnetic axis (upper trace) and the other near the pedestal top (lower trace) (the integration lengths of core and edge probing beams are  $\sim 3.2\text{m}$  and  $\sim 1.5\text{m}$ , respectively), (e) electron temperature in the core and near the pedestal top, (f) H98Y, estimated based on the measured total stored energy, (g) the  $D_\alpha$  signal measured at the inner divertor. The pulse had a toroidal magnetic field of  $B_t = 1.78\text{ T}$  and a plasma current of  $I_p = 1.5\text{MA}$ , corresponding to an edge safety factor of  $q_{95} = 4.0$ . In these experiments, the type-I ELMy H-mode plasma with a high triangularity shape ( $\delta_U = 0.45$  and  $\delta_L = 0.4$ ) was sustained by Neutral Beam Injection (NBI) with a input power of  $9.2\text{MW}$  for  $6\text{s}$ . The electron collisionality at the pedestal is  $\sim 0.2$ . No additional gas fuelling was applied during the H-mode phase. The  $n = 1$  perturbation field created by the EFCCs has a at top with  $I_{\text{EFCC}} = 24\text{kA}$ t for  $3\text{s}$ , which is by a factor of  $\sim 10$  longer than the energy confinement time of this pulse. Here, the EFCC coil current is only limited due to the  $12\text{t}$  thermal rating limit of the power supplies.

During the EFCC phase, the  $D_\alpha$  signal (g) measuring the ELMs showed a strong reduction in amplitude. The ELM frequency increased from  $\sim 10\text{Hz}$  to  $\sim 40\text{Hz}$ , while the periodic change in  $T_e$  at the edge pedestal due to the ELM crashes,  $\Delta T_e$ , reduced from  $\sim 600\text{eV}$  to  $\sim 150\text{eV}$  measured by the ECE diagnostic. The energy loss per ELM normalized to the total stored energy,  $\Delta W/W$ , measured by the fast diamagnetic loop indicates a strong reduction from  $\sim 6\%$  to values below the noise level ( $< 2\%$ ) of the diagnostic. A continuous decrease in the electron density is observed in the core and edge line-integrated electron density signals even during the flat-top of  $I_{\text{EFCC}}$ . A modest drop (a few percent) in the total stored energy during the ELM mitigation phase with the EFCCs due to the strong density pump-out effect occurs, the plasma confinement quality (H98Y) is not reduced. This is mainly due to the energy confinement time for a ELMy H-mode plasma which scales with  $n_e^{0.41}$  [1].

The changes of the plasma profiles are shown in Fig. 3 (a and b). The electron density decreases everywhere by  $\sim 24\%$  during the application of the  $n = 1$  EMPFs, this is the so-called pump-out effect. However, the electron temperature increased from  $3.2$  to  $4.3\text{keV}$  at the plasma core and from  $1.1$  to  $1.5\text{keV}$  at the pedestal. The pedestal ion temperature also increased from  $1.4$  to  $1.7\text{keV}$ . The electron collisionality at the pedestal dropped down to  $\sim 0.08$ .

### 3.2. DEPENDENCE OF ELM MITIGATION WITH $n = 1$ EMPF ON $q_{95}$

Results from DIII-D have shown, that with the  $n = 3$  perturbation field the edge safety factor was a crucial quantity and complete ELM suppression was only achieved within a narrow range [5]. In the JET experiments, ELM mitigation with the  $n = 1$  EMPFs are performed at different  $q_{95}$  of  $4.8$ ,  $4:0$ ,  $3:5$  and  $3.0$  by changing the values of the plasma current to  $1.4$ ,  $1.6$ ,  $1.8$  and  $2.0\text{MA}$  and keeping the same toroidal magnetic field of  $1.84\text{ T}$ . ELM mitigation was achieved for all values of  $q_{95}$  as shown in Fig.4 (a–d). When the EFCC coil current increased above the critical value,  $I_{\text{ELM}}^{\text{min}}$ , the ELM frequency

started to increase while the drop in  $T_e$  during the ELM collapse,  $\Delta T_e$ , decreased. The minimum EFCC current for ELM mitigation increased with decreasing  $q_{95}$ , but always remained below the  $n = 1$  locked mode threshold as shown in Fig.5.

A further increase of  $I_{\text{EFCC}}$  actively controlled both,  $f_{\text{ELM}}$  and  $\Delta T_e$ . With  $I_{\text{EFCC}} = 36.8\text{kAt}$ , the ELM frequency in the pulses with  $q_{95}$  of 4.8 and 4.0, increased from  $\sim 35\text{Hz}$  to  $\sim 190\text{Hz}$  and from  $\sim 30\text{Hz}$  to  $\sim 125\text{Hz}$ , respectively. However, the dependence of  $f_{\text{ELM}}$  on  $I_{\text{EFCC}}$  is found to be different between ramp-up and ramp-down of  $I_{\text{EFCC}}$  as indicated in Fig. 4 (a) and (b) which could be due to a hysteresis effect or non-stationary nature of the experiment. In the cases of  $q_{95} = 3.5$  and  $3.0$ , the ELM frequency increased quickly by a factor  $\sim 4$  from  $\sim 20\text{Hz}$  to  $\sim 80\text{Hz}$  before the locked mode threshold was reached.

#### 4. ELM MITIGATION WITH $N = 2$ EMPF

The first experiments of ELM mitigation using  $n = 2$  EMPFs induced by the EFCCs have been carried out on JET. Figure 6 (left) shows the time evolution of  $I_{\text{EFCC}}$ ,  $f_{\text{ELM}}$ ,  $\Delta T_e$ , and the drop of electron density due to the pump-out effect of the EMPFs,  $\delta n_e$ , for a discharge with  $I_p = 1.6\text{MA}$ ,  $B_t = 1.85\text{T}$  and  $q_{95} = 4.0$ . In this experiments, the EFCC current has been limited to values below  $24\text{kAt}$  which is 65% of the  $n = 1$  case. This was due to a technical limitation of the EFCCs power supply system on JET.

In the shown pulse, the  $I_{\text{min}}$  ELM observed is  $\sim 16\text{kAt}$  which is similar to that with the  $n = 1$  EFCCs (see Fig. 4 (c)). Further increase of  $I_{\text{EFCC}}$  up to  $24\text{kAt}$  results in an increase in  $f_{\text{ELM}}$  from  $15\text{Hz}$  to  $40\text{Hz}$ , and a reduction in  $\Delta T_e$  from  $650\text{eV}$  to  $\sim 250\text{eV}$ . A continuous drop in the plasma density has been observed even after the flat top of  $I_{\text{EFCC}}$  was approached. On JET, the wiring of the  $n = 2$  EFCCs allows only two different phases depending on the current direction in the coil pairs. The pump-out effect, the reduction in ELM amplitude, and the simultaneous increase in ELM frequency were observed with both phases. However, one phase has been identified where the application of the  $\bar{n}$ -field perturbation leads to a slight shrinking of the plasma column due to the action of the plasma position and boundary feedback control because the magnetic pick-up coils measure the applied perturbation field. This effect is similar to the  $n = 1$  configuration [13].

The dependence of the ELM mitigation with  $n = 2$  EMPF on the edge safety factor,  $q_{95}$ , was also investigated. In these experiments,  $q_{95}$  was varied between 3.1 and 4.5 by choosing different plasma currents of  $I_p = 1.6, 1.25$  and  $1.1\text{MA}$  with the same magnetic field of  $1.6\text{T}$ . ELM mitigation was achieved for all values of  $q_{95}$  as show in Fig. 6. The ratios of the ELM frequency with and without application of the  $n = 2$  perturbation field are  $10\text{Hz}/18\text{Hz}$ ,  $10\text{Hz}/35\text{Hz}$  and  $15\text{Hz}/38\text{Hz}$  for the  $q_{95}$  of 3.1, 4.0 and 4.5, respectively. No locked mode was excited by the  $n = 2$  EFCCs.

#### DISCUSSION AND CONCLUSION

An increase in  $f_{\text{ELM}}$  has been observed when an  $n = 1$  magnetic perturbation field was applied. This observation is different from the results from DIII-D, where the type-I ELMs were completely suppressed with an  $n = 3$  resonant magnetic perturbation. The density pump-out effect and the changes

in the edge temperature profile are similar [5]. On DIII-D, the magnetic perturbation spectrum induced by internal coils with an  $n = 3$  configuration is very sharp, which can explain partly the narrowness of the  $q_{95}$  window for complete ELM suppression. However, the EFCCs with a low  $n$  (1 or 2) configuration on JET, produce a broad magnetic perturbation spectrum. The influence of the  $q$  profile on the resonant components at the various rational surfaces induced by the magnetic perturbation is not very large. This is consistent with the experimental observation of a wide  $q_{95}$  window for ELM mitigation with  $n = 1$  and  $n = 2$  EMPFs on JET.

During the application of the  $n = 1, 2$  EMPFs, a reduction in the ELM size ( $\Delta W$ ) and ELM peak heat °fluxes on the divertor target by roughly the same factor [18] as the increase of the ELM frequency has been observed. The reduction in heat flux is mainly due to the drop of particle flux rather than the change of the electron temperature. Here, the heat fluxes are measured by both, Langmuir Probes embedded in the divertor tiles and a fast IR camera viewing the divertor targets. In addition, the results from the Quartz MicroBalance (QMB) [19] measuring the amount of carbon deposited in the inner divertor louver indicates clearly less erosion of carbon on the divertor with mitigated ELMs. In type-I ELMy H-mode plasmas, net-deposition of carbon on the QMB with a growth rate of  $\gg 0.6\text{nm/s}$  was observed. However, when the large ELMs were mitigated by  $n = 1$  EMPFs, net-erosion of carbon from the QMB ( $\sim 0.25\text{ nm/s}$ ) was observed, which is mainly due to a strong reduction of the carbon flux but still having a significant deuterium flux.

A strong braking of the toroidal plasma rotation [20] has been observed during the ELM mitigation with either the  $n = 1$  or the  $n = 2$  EMPFs. When the  $n = 1$  EMPF was applied, the frequency of the sawtooth precursor mode,  $f_{ST}^{PC}$  at in the plasma core was reduced from 10kHz to 6kHz when the  $I_{EFCC}$  increased up to 24kAt. There is a critical value of the  $I_{EFCC}$  observed above which the  $f_{ST}^{PC}$  started to decrease. The changes of  $f_{ST}^{PC}$  are linearly dependent on the amplitude of the  $I_{EFCC}$  after the critical value ( $\sim 12\text{kAt}$ ) of the  $I_{EFCC}$  has been exceeded. Since the amplitudes of both  $n = 1$  and 2 harmonics in  $n = 2$  EFCC configuration are by a factor of 4 smaller than that of  $n = 1$  harmonic in  $n = 1$  EFCC configuration as shown in Fig.1 (right), this indicates that non-resonance magnetic braking could play a role in the influence on the plasma rotation.

In conclusion, active control of type-I ELMs with  $n = 1$  EMPFs has been developed for more ITER-relevant configurations and parameters in a wide operational space of plasma triangularity,  $q_{95}$  and beta on JET. The frequency of ELMs increased by a factor of 4 for a duration of 10 times the energy confinement time in a high triangularity plasma, while the energy loss per ELM,  $\Delta W=W$ , decreased from 6% to below the resolution limit of the diamagnetic measurement ( $\sim 2\%$ ). A reduction in ELM peak heat fluxes on and carbon erosion of the divertor target plates has been observed during the ELM mitigation with the  $n = 1$  EMPFs. The first results of ELM mitigation with the  $n = 2$  EMPFs on JET demonstrate that the frequency of ELM can be increased from 10Hz to 35Hz even with a limited EFCC coil current of 24kAt. A wide operational window of  $q_{95}$  has also been obtained for ELM mitigation with  $n = 2$  EMPFs.

## REFERENCES

- [1]. ITER Physics Basis, Nuclear Fusion **39** 2137 (1999).
- [2]. F. Wagner et al , Phys. Rev. Lett. **49**, 1408 (1982).
- [3]. J.W. Connor, Plasma Phys. Control. Fusion **40**, 531 (1998).
- [4]. A. Loarte et al , J. Nucl. Materials **313-316**, 962 (2003).
- [5]. T. Evans et al , nature physics **2**, 419 (2006).
- [6]. P.T. Lang et al , Nucl. Fusion **44**, 665 (2004).
- [7]. A. W. Degeling et al , Plasma Phys. Control. Fusion **45**, 1637 (2003).
- [8]. V. Parail et al , ECA 29C, O-2.008 (2005).
- [9]. M. Mori et al , Plasma Phys. Control. Fusion **38**, 1189 (1996).
- [10]. S.J. Fielding et al , ECA 25A, 1825 (2001).
- [11]. T. Evans et al , Phys. Rev. Lett. **92**, 235003 (2004).
- [12]. I. Barlow et al , Fusion Eng. Des. **58-59**, 189 (2001).
- [13]. Y. Liang et al , Phys. Rev. Lett. accepted for publication, (2007).
- [14]. R.V. Budny et al , Nucl. Fusion **35**, 1497 (1995).
- [15]. J.C. Vallet, et al , Phys. Rev. Lett. **67**, 2662 (1991).
- [16]. H.R. Koslowski et al , 34th EPS, P5.135 (2007).
- [17]. R. J. Buttery et al , Nucl. Fusion **39**, 1827 (1999).
- [18]. S. Jachmich et al , 34th EPS, P5.099 (2007).
- [19]. H.G. Esser et al , J. Nucl. Materials **337-339**, 84 (2005).
- [20]. E. Lazzaro et al , Phys. Plasmas **9**, 3906 (2002).

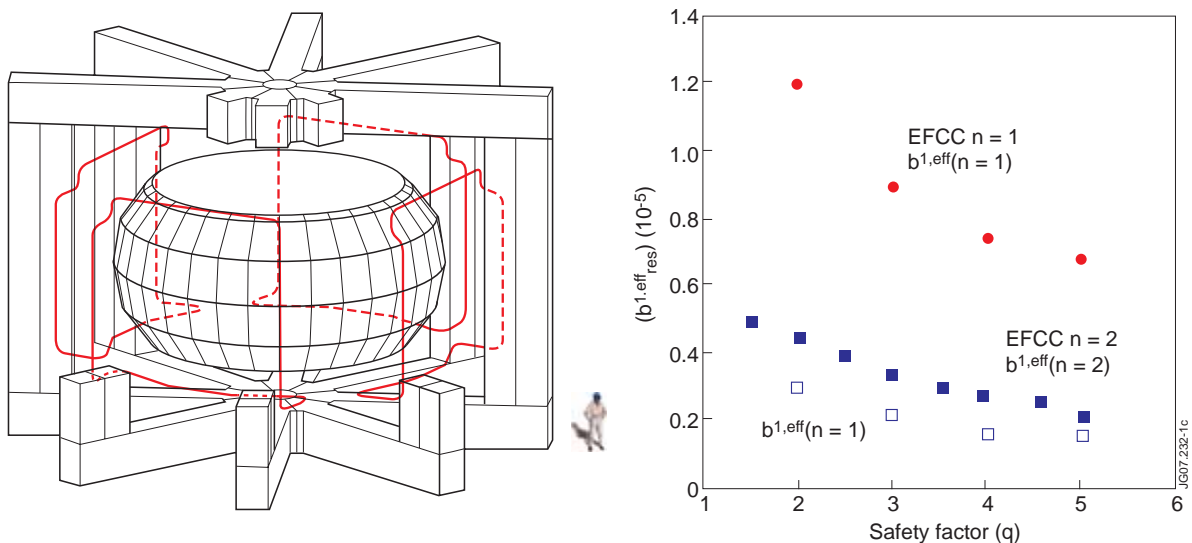


Figure 1: (a) Perspective view of JET showing the 4 large error field correction coils mounted between the transformer limbs. (b) Effective resonant magnetic perturbation for 1kAt in the EFCCs in  $n = 1$  and  $n = 2$  configurations.

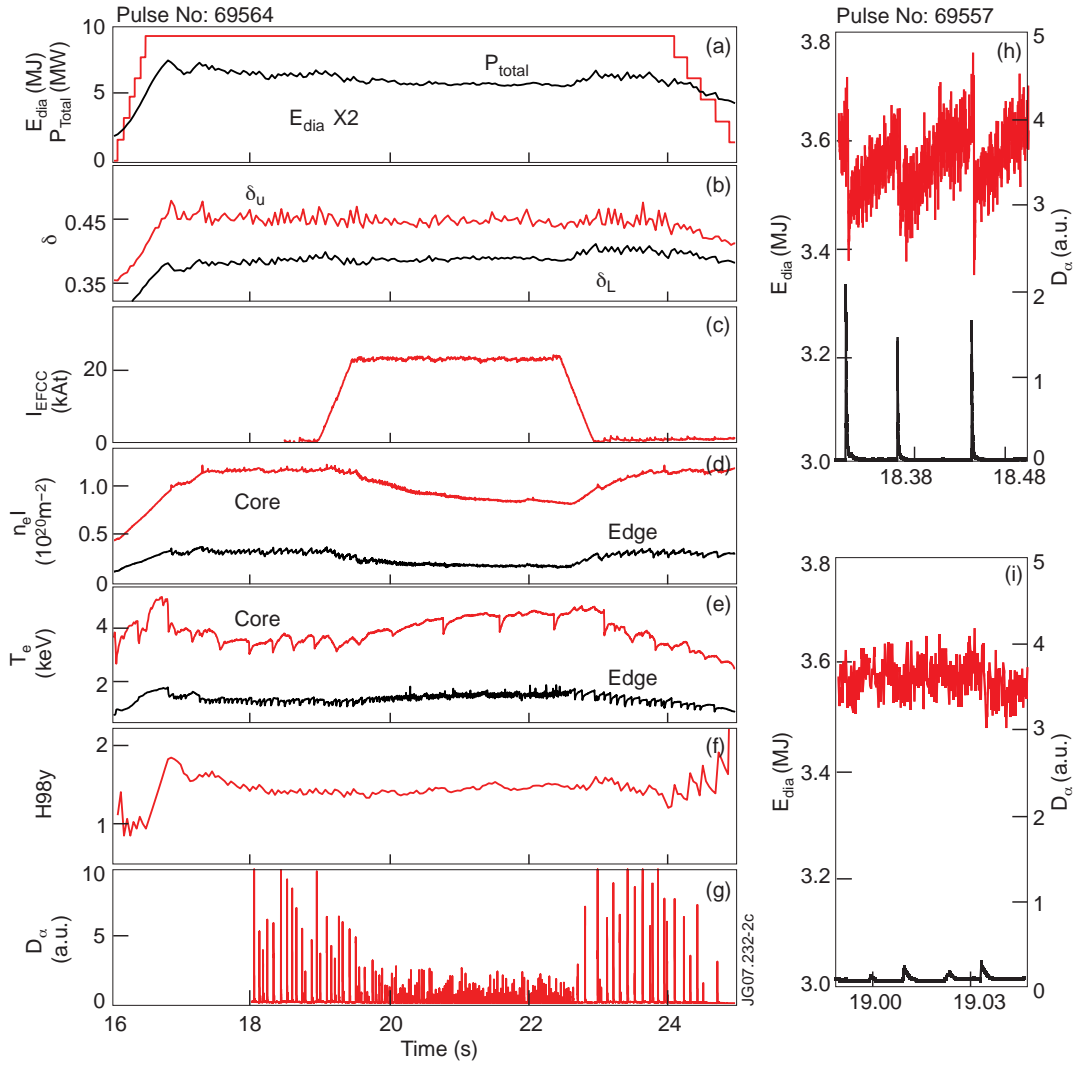


Figure 2: (a–g) Overview on a typical ELM mitigation experiment in a high triangularity plasma on JET. The time traces of the total stored energy,  $E_{dia}$  and the intensity of the Da lines measured before (h), and during (i) ELM mitigation with the  $n = 1$  EFCCs are from a discharge similar to the one shown in (a–g).

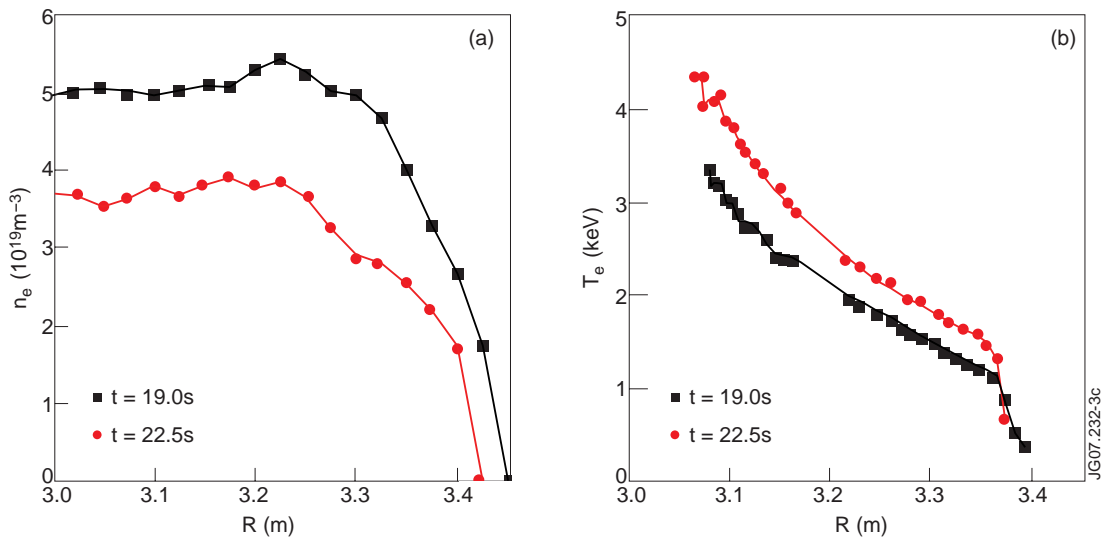


Figure 3: The profiles of (a) electron density and (b) electron temperature in the discharge shown in Fig.2 at times before (+) and during (o) the  $n = 1$  EFCC applied. All profiles are mapped onto the plasma midplane.

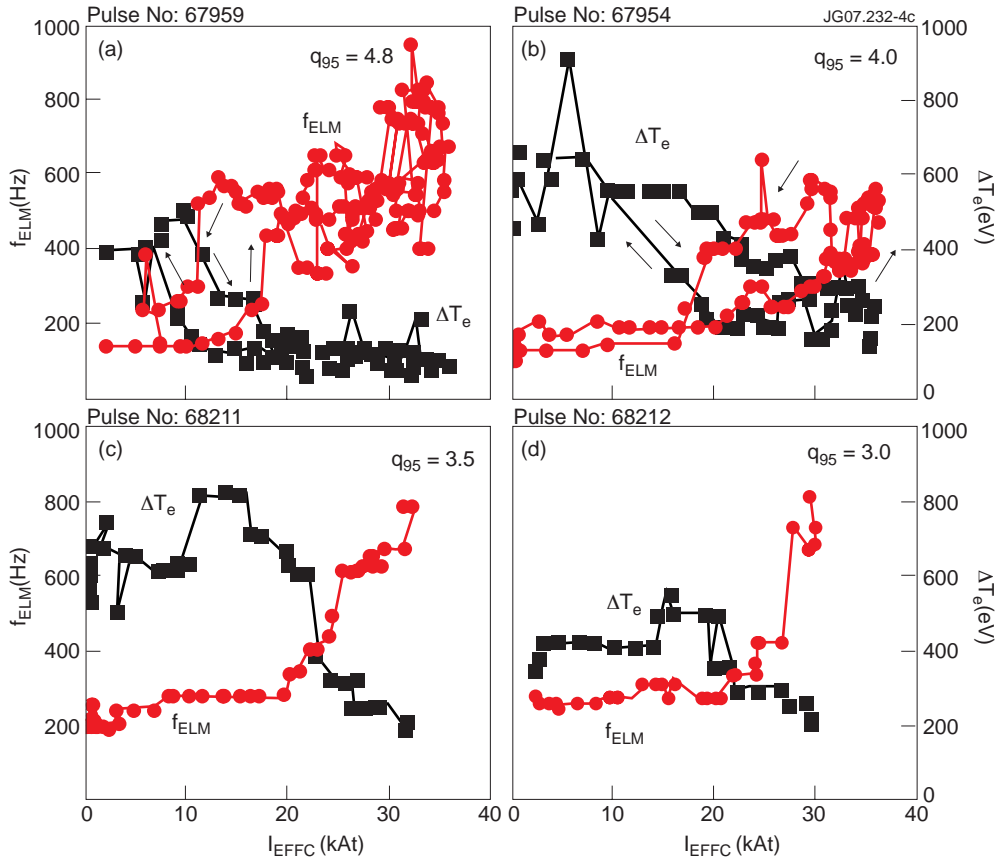


Figure 4: Frequency of the ELMs,  $f_{ELM}$ , and the amplitude of  $\Delta T_e$  as a function of  $I_{EFCC}$  in discharges with different edge safety factor,  $q_{95}$ , of 4.8 (a), 4.0 (b), 3.5 (c) and 3.0 (d).

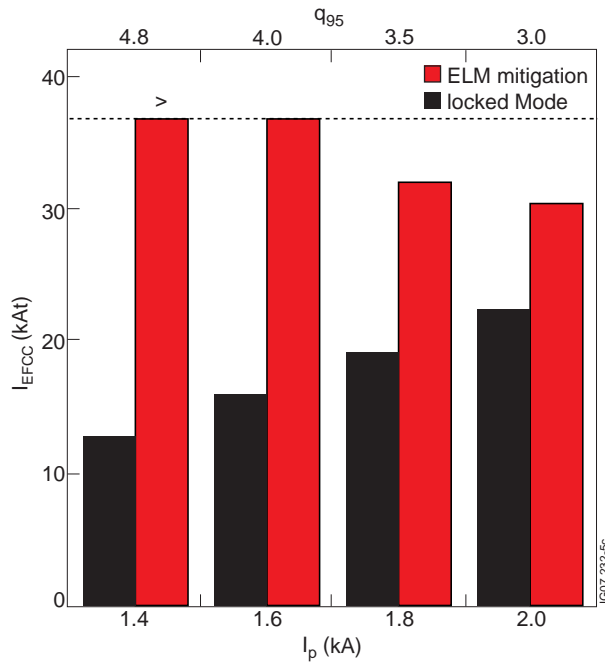


Figure 5: The minimum EFCC coil currents,  $I_{EFCC}$ , for ELM mitigation (left bar) and excitation of a locked mode (right bar) as a function of plasma edge safety factor,  $q_{95}$ .

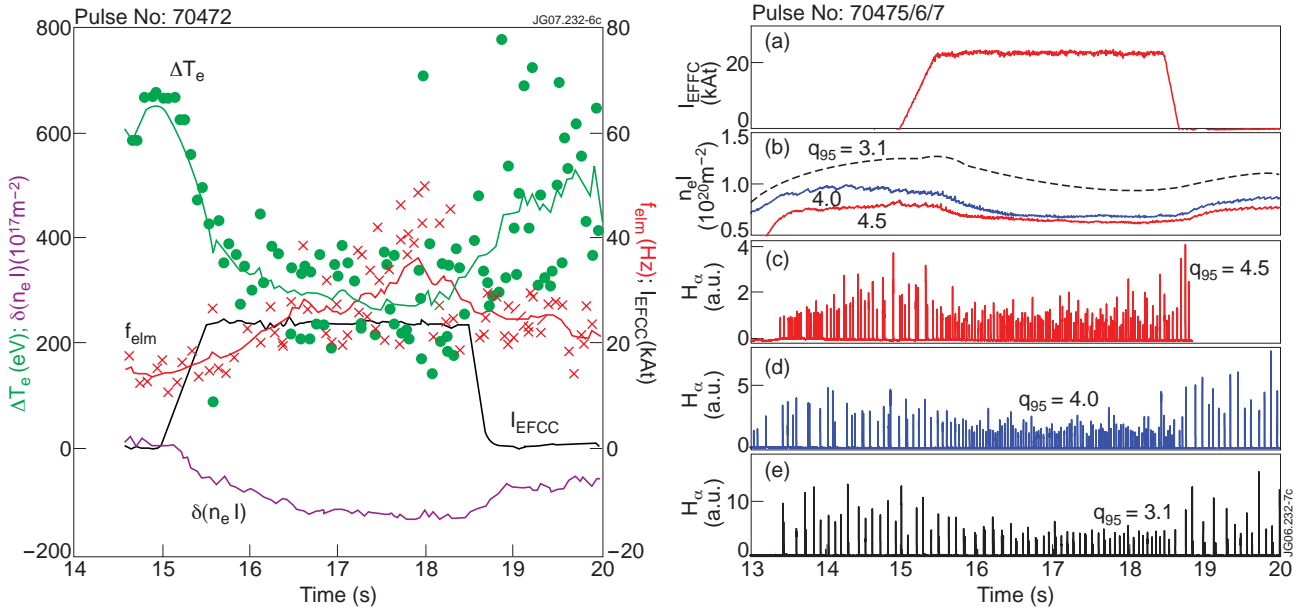


Figure 6: (left) Time evolution of  $I_{EFCC}$ ,  $f_{ELM}$ ,  $\Delta T_e$ , and  $\delta n_e$  for a discharge of ELM mitigation with the  $n = 2$  EFCCs on JET. (right) Time trace of (a)  $I_{EFCC}$ , (b)  $n_e l$ ,  $D_{\alpha}$  measured from the plasmas with different  $q_{95}$  of (c) 4.5, (d) 4.0 and (e) 3.1.